NUEJ
Naresuan University Engineering Journal

New Classification of Textile Samples through l_p Norm Spectral Enhancement Using Template Filters Combining the Analytic Geometry Technique

Wachira Limsripraphan, Suchart Yammen*

Department of Electrical and Computer Engineering, Faculty of Engineering, Naresuan University, Phitsanulok, Thailand

*Corresponding author e-mail sucharty@nu.ac.th

(Received: 3 November 2023, Revised: 27 November 2023, Accepted: 1 December 2023)

Abstract

This paper introduces a novel method for classifying textile fibers into three groups: natural fibers, synthetic fibers, and blended fibers using near-infrared (NIR) spectra obtained via the NeoSpectra-Micro sensor. Our approach involves preprocessing and employing the l_p-norm with p = ∞, 1, and 2 to enhance spectral signals. These enhanced signals alongside textile template filters were obtained from both natural and synthetic fiber groups. Next, the template filters are used to construct a new 2x1 feature vector through covariance-based techniques to effectively reduce spectral data dimension. The feature vector is pivotal for establishing two threshold lines together with an analytical geometry technique to classify for accurate fiber groups. To evaluate the performance of the proposed method, experiments were conducted by using three groups of fiber samples: 210 natural fiber spectra, 480 synthetic fiber spectra, and 270 blended fiber spectra. The dataset was divided into training and testing sets with ten random iterations exploring eight ratios and l_p-norm enhancements for training and evaluation. Remarkably, the experimental result has shown that the overall accuracy remains consistent across the three cases of the l_p-norm enhancements providing the similar accuracies. Considering the limited computational resource, the l_1-norm emerges as a practical choice for embedded systems, emphasizing its practicality for implementation. Moreover, the proposed method additionally provides high accuracies (mean ± standard deviation) of 0.9995 ± 0.0006, 0.9999 ± 0.0004, and 0.9999 ± 0.0005, whereas the ratio of the train and test data is equal to three cases: 10:90, 20:80 and 30:70, respectively, and achieves an exceptional overall accuracy of 100%, whereas the ratio of the train and test data is equal to five cases: 40:60, 50:50, 60:40, 70:30 and 80:20.

Keywords: l_p norm Enhancement, Near-Infrared (NIR) spectroscopy, Template Filters, Textile Fiber Classification

1. INTRODUCTION

The textile industry is one of the most polluting industries, primarily due to its manufacturing processes that extensively use the second highest amount of land resources and the fourth highest amount of water resources. It contributes to greenhouse gas emissions and water pollution, accounting for 10% and 20% of the global world's pollution, respectively (Dissanayake & Weerasinghe, 2021; Filho et al., 2022). Additionally, global post-consumer textile waste has nearly doubled from 58 million to 109 million tons per year in the past decade, leading to issues to textile waste in landfills and contributing to microfiber pollution in oceans.

Recycling textile waste is an important approach to make the textile industry more sustainable and move towards a circular economy. However, only 1% of textile waste can be currently recycled into new clothing due to technological limitations in efficiently and rapidly classifying different fiber components. This is because the fiber composition in textiles, such as polymer fibers in synthetic fabrics and cellulose fibers in natural fabrics, or blended fabrics containing both types, requires different recycling methods (Damayanti et al., 2021; Piribauer & Bartl, 2019).

In recent year, near-infrared (NIR) spectroscopy has become a popularity as a method for textile analysis and classification due to its ease of use, non-destruct the samples, efficiency, cost-effectiveness, and time-saving advantages compared to traditional laboratory-based chemical analysis methods (Guifang et al., 2015; Sun et al., 2015; Chen et al., 2018). However, it is essential to highlight that in the majority of research applications, preprocessing and dimensionality reduction steps are prerequisites before developing classification models. Similarly, alternative methods using low-cost devices, such as image processing, have emerged as viable options for textile classification, as demonstrated by Da Silva Barros et al. (2020). Their approach involves the utilization of mobile device images and Convolutional Neural Networks (CNN) for feature extraction. The

experimental results indicate that feature extraction using DenseNet201 and the SVM classification model achieved the highest accuracy, with an accuracy rate of 94.350% and an F1-Score of 94.296%. This underscores the importance of employing robust feature extraction techniques in both NIR spectroscopy and image processing for accurate textile classification.

Wu et al. (2015) employed preprocessing techniques, including the first derivative and the standard normal variant (SNV), before applying the principal component analysis (PCA), a widely used method for linear dimensionality reduction. This approach generated six principal components (PCs), which subsequently served as input variables for a classification model based on least-squares support vector machines (LS-SVM). The LS-SVM model was utilized to classification four types of natural fibers. Sun et al. (2015) employed the Savitzky-Golay first derivative with a five-point window width as preprocessing and used PCA to reduce the initially high dimensionality of 3,000 variables per NIR spectra from the Antaris II FT-NIR spectrometer. They reduced these variables to 3, 4 and 6 PCs, which were used as new input variables for SIMCA analysis, LS-SVM with the RBF kernel function, and the extreme learning machine (ELM) model to classify various fabrics, including cotton, viscose, acrylic, polyamide, polyester, and blend fabric. The results indicated that ELM model achieved a 100% with higher processing speed compared to SIMCA and LS-SVM. Zhou et al. (2019) applied the second derivative as preprocessing before used PCA to reduce 601 variables per NIR spectra obtained from the Brimrose Luminar 3060 AOTF-NIR to three PCs. The new variables were subsequently used in SIMCA analysis to classify seven types of fabric into three groups. The results indicated that PP, PET, PLA, cotton and tencel fabrics were accurately classified with almost perfect accuracy of 100%, whereas wool and cashmere fabrics required another method to achieve best classification accuracy of 100%, specifically the linear discriminant analysis (LDA).

Recently, Ruiz et al. (2022) aimed to enhance the accuracy of classifying post-consumer textile waste by employing data fusion techniques that combined MIR (mid-Infrared) and NIR (near-Infrared) spectroscopy data. Before fusing the given data, they conducted a preprocessing step, which involved applying the first and second derivatives of the Savitzky-Golay smoothing method with a moving average window of 5 and 10 points. They additionally performed mean-centering and balanced the weight of the MIR and NIR spectra data within the 0–1 interval by using min-max normalization. For dimensionality reduction, they utilized the PCA and the canonical variate analysis (CVA) to reduce the dimensionality of the fusion data, which consisted of 3,551 variables from MIR and 2,201 variables from NIR. This reduction produced a new set of variables equal to the number of classes minus one. Subsequently, these new variables served as inputs for a k-Nearest Neighbors (kNN) classification model. The results indicated that the fusion data provided more accurate classification results than using the NIR or MIR spectra data separately, particularly in the case study of blended fibers (mixed between cotton fibers and polyester fiber) achieving the best accuracy with only a 5% error in classification, whereas the error rates for the NIR and MIR spectra were 7% and 6%, respectively. In the same year, Ruiz, Cantero, Riba-Mosoll, et al. (2022) employed a Deep Learning algorithm based on convolutional neural networks (CNNs) to classify textile waste, which included both pure fibers and cotton/polyester blend fibers. They proposed two distinct methods in their methodology both beginning with crucial preprocessing steps involving the calculation of the first or second derivatives and mean-centering of the NIR spectrum. In the first approach, no dimensionality reduction step was applied before the CNN classification. In contrast, the preprocessed spectral data underwent transformation using the PCA and CVA algorithms to reduce dimensionality and create new variables for the classification step alongside the CNN in the second approach. The results demonstrated that the PCA + CVA + CNN approach in the second method outperformed the CNN-only method without dimensionality reduction. Specifically, the PCA + CVA + CNN approach achieved a correct classification rate of 100% in the case study of pure fibers and a correct classification rate of 91.1% in the case study of cotton/polyester blend fibers.

From all the research reviewed above, it is evident that preprocessing processes with a variety of methods such as standard normal variables (SNV), and first or second derivatives combined with Savitzky-Golay smoothing, and widely used dimensionality reduction processes like PCA, are essential for achieving accurate textile classification with NIR data. This finding aligns with our previous research (Limsripraphan & Yammen, 2022), which demonstrated that preprocessing processes with signal enhancement in proposed methods improved the classification efficiency. In addition, it has been shown that improving the accuracy of blended textile classification using NIR spectra remains a major challenge.

This paper presents a novel classification approach to classifying textile samples. The method involves

several key steps, starting with $l_p - norm$ spectral enhancement as a preprocessing technique (Cadzow, 2002; Cadzow et al., 2002) and utilizing covariance-based feature filters (Yammen et al., 2021) for dimensionality reduction to extract a useful feature vector. Subsequently, this new feature vector is subjected to the analytic geometry (AG) technique to establish threshold lines that can classify textile fibers into three groups: natural, synthetic, and blended fibers. The performance of the classifiers is evaluated using three key metrics: overall accuracy, precision, and recall. These metrics are also applied to various scenarios, considering different cases of $l_p - norm$ spectral enhancement, where p takes on values of $1, 2, \infty$ across varying training and testing dataset ratios. The proposed method consistently achieves overall accuracy of 100% for all $l_p - norm$ spectral enhancement, even when the training dataset is reduced unto 30%, which differs from the observed variations in accuracy under different training and testing data ratios.

In conclusion, this paper aims to highlight the improvement in the accuracy of the textile classification using the NIR spectra, particularly in classifying blended fabrics and reducing intensive computational resources. The objective is to employ simple and interpretable methods while comparing the effectiveness of $l_p - norm$ spectral enhancement in achieving best classification accuracy.

2. SPECTRA DATA PREPARATION

2.1 Sample Collection and Identification

The NIR spectral data in this paper were collected from samples of various types of woven and knitted fabrics commonly used in clothing production. These samples were sourced from fabric distributors and factories in Thailand. The textile samples include natural fibers (such as cotton, linen, and rayon), synthetic fibers (like polyester or spandex) and blended fibers between both types in various proportions from high to low ratios of natural to synthetic fiber. Additionally, to include maximum variability in the analyzed set of samples, each fabric sample was selected in a multitude of colors ranging from dark to light.

All fabric samples were sent to the textile testing center, Thailand's textile institute (THTI), which operates under the Ministry of Industry's Foundation for Industrial Development (FID), to confirm the fiber composition and to identify the fabric samples into three groups. The fiber composition was determined based on the clean dry mass with percentage additions for moisture method under the Thai Industrial Standard (TIS), Standards No.121 part 26-2552. This method is widely recognized for quantifying binary mixtures of fibers in textile products.

In summary, all fabric samples were categorized into three fiber group based on the composition confirmed by THTI: 7 fabric types in natural fiber group, 16 fabric types in synthetic fiber group, and 9 fabric types in blended fiber group, which were further divided into 7 different ratios of natural to synthetic fiber: 68:32, 52:48, 48:52, 36:64, 35:65, 34:66, and 17:83. There are total 32 fabric types, and each of which comes in 3 different colors. Therefore, this research utilized a total of 96 fabric samples for training and testing the performance of the proposed method.

2.2 NIR Spectral Acquisition

The NIR spectra of the textile samples were acquired using the NeoSpectra-Micro Development Kit (Si-ware Systems, Cairo, Egypt), a portable NIR instrument that has shown its reliability for analysis and classification in various fields. These fields include food (McVey et al., 2021; Giussani et al., 2021; Chadalavada et al., 2022), healthcare (Habibullah et al., 2019), agriculture (Du et al., 2019), and textile fibers as shown in a previous study (Yammen et al., 2022; Limsripraphan. et al., 2022; Cadzow, 1999). The device is housed in a specially designed enclosure to prevent interference from external light and to maintain consistent measurements over fabric samples at a height of one centimeter as shown in Figure 1.

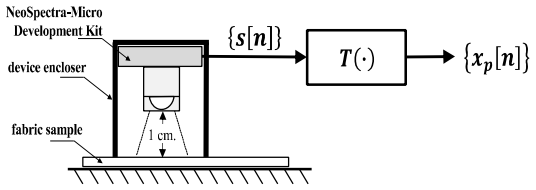

Figure 1 NIR spectral acquisition and spectral enhancement

Each spectral value is acquired using a device that records data for 65 pairs of absorbance and wavelength in the range of 1350 nm to 2550 nm. This data is then transformed in the form of signals representation $\{s[n]\}$, where $n \in \{0,1,2,\dots,64\}$, as shown in Figure 2. All fabric samples are measured at 10 positions on a fabric sample with dimensions of 30 x 50 centimeters. Therefore, 960 NIR spectral samples were obtained for use in the proposed method.

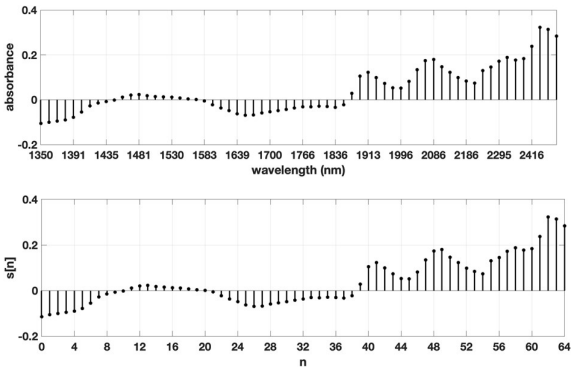

Figure 2 NIR spectral signals representation

2.3 NIR Spectral Signal Enhancement with l_p norm

Before applying our proposed classification method to the 960 NIR spectral samples, we introduce $l_p - norm$ spectral enhancement (Cadzow, 1998) as a preprocessing step to reduce the spectral variability of the input spectral signals $\{s[n]\}$ (Bunchuen et al., 2011). In this process, each spectral signal is normalized by subtracting its mean and dividing the result by its l_p norm, resulting in an enhanced spectral signal $\{x_p[n]\}$ as calculated using Eq. (1). We explore various p values to assess their impact on classification accuracy when applying our proposed method in section 4.

$$x_p[n] = T(\{s[n]\}) = \frac{s[n] - \mu_s}{\|\{s[n] - \mu_s\}\|_p}\ , \qquad (1)$$

where: p = 1, 2, ∞ and

$$\mu_s = \frac{1}{65}\sum_{n=0}^{64} s[n] \qquad (2)$$

2.4 Train and Test Datasets

In this study, the entire set of enhanced spectral signals $\{x_p[n]\}$, obtained from three enhancement studies using $l_p - norm$ with p values of 1, 2, and ∞ was randomly divided into eight different proportions for the train-to-test dataset within each fiber group. These proportions included 10:90, 20:80, 30:70, 40:60, 50:50, 60:40, 70:30, and 80:20, as shown in Table 1.

This approach allowed us to assess the accuracy of our proposed classification method, which was trained using the train dataset, while ensuring that the testing data were not used during the training step. Additionally, this evaluation helped us understand the performance of our proposed method when the amount of training data is reduced. Moreover, each sample was labeled to identify its respective fiber group, facilitating the assessment of correct classification.

Table 1 Number of Train and Test Samples

proportions	Train dataset			Test dataset		
	Natural (N_n)	Synthetic (N_s)	Blended (N_b)	Natural (N_n)	Synthetic (N_s)	Blended (N_b)
10:90	21	49	27	189	432	243
20:80	42	96	54	168	384	216
30:70	63	144	81	147	336	189
40:60	84	192	108	126	288	162
50:50	105	240	135	105	240	135
60:40	126	288	162	84	192	108
70:30	147	336	189	63	144	81
80:20	168	384	216	42	96	54

3. METHODOLOGY

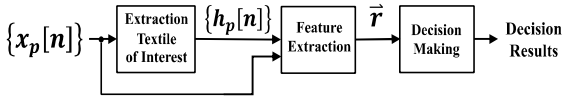

Figure 3 Diagram of proposed classification method

Figures 3 shows our proposed method for classifying textile fibers into three groups. We utilize enhanced spectral signals $\{x_p[n]\}$ as input to extract patterns of interest in natural and synthetic fiber spectra, resulting in the creation of two textile template filters. These template filters are then employed for feature extraction based on covariance, leading to the creation of the two new feature vectors. Each of the two feature vectors is utilized to build a classification system that facilitates decision-making regarding fiber groups.

3.1 Textile Template Filter

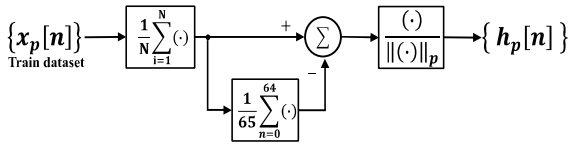

Figure 4 Diagram of create textile templates filter

In this section, we introduce to creation of textile template filter to extract characteristic patterns of interest within in either natural or synthetic fibers spectra group. To create this filters, we start by utilizing input data of interest derived from the training dataset. We computed the average of the enhanced spectral signals $\{x_p[n]\}$, which serves as the input. This average spectrum was then normalized by subtracting its mean and dividing the result by its $l_p - norm$, resulting in the textile template filters $\{h_p[n]\}$ as shown in Figure 4. Consequently, when we utilize spectra from the training dataset of the natural

group ($N = N_n$ samples), the textile template filters represent the pattern within natural fiber spectra. Similarly, when employing spectra from the synthetic group ($N = N_s$ samples), the textile template filters represent the pattern within synthetic fiber spectra.

3.2 Feature Extraction with Covariance-based

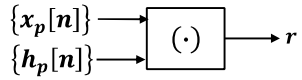

Figure 5 Diagram of covariance-based feature

The proposed method involves a dimensionality reduction process by extracting useful features using the textile template filters $\{h_p[n]\}$, which effectively represent characteristic patterns in natural or synthetic fiber groups. We employ a covariance-based technique (Fuangpian et al., 2011) to assess the similarity between two inputs: the enhanced spectral signals $\{x_p[n]\}$ from unknown fiber groups and the representations of natural or synthetic fiber spectra provided by the textile template filters $\{h_p[n]\}$. This process results in a r value as shown in Figure 5, within the interval from 0 to 1 described in Eq. (3), signifying the degree of similarity.

$$r = \frac{\sum_{l=0}^{64} x_p[l]h_p[l]}{\|\{x_p[n]\}\|_2 \times \|\{h_p[n]\}\|_2} \;;\; 0 \le r \le 1 \qquad (3)$$

When employing textile template filters from the natural fiber group and utilizing enhanced spectral signals $\{x_p[n]\}$ from the unknown fiber groups as input, the resulting r values, denoted as r_n, indicate a high degree of similarity to the patterns found in natural fiber spectra. Similarly, when employing textile template filters from the synthetic fiber group with the same input enhanced spectral signals, the resulting r values, denoted as r_s, signify patterns highly similar to those present in synthetic fiber spectra. These values are pivotal in our approach as they form the foundation of the new feature vector denoted as a 2x1 feature vector $\vec{r}$ with r_n and r_s as its components. This transformation practically reduces feature dimensionality from 65 to 2, ensuring efficient separation and classification of textile fibers based on their spectral. This new feature vector $\vec{r}$ is used for analysis to create our proposed classification algorithm, which utilizes the analytic geometric technique as shown in Figure 6.

3.3 Classification Algorithm using Analytic Geometric technique

Figure 6. shows a scatter plot of all two-dimensional vectors $\vec{r}_i$ obtained from the training dataset, comprising three distinct fiber groups, where $i \in \{1,2,3,\dots,N\}$. Each vector is represented as an ordered pair (r_{ni}, r_{si}), with r_{ni} denoted the x-axis component and r_{ni} representing the y-axis component.

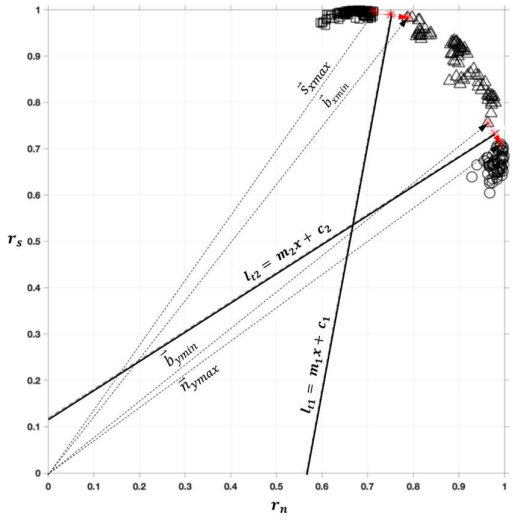

Figure 6 Classification using Analytic Geometric technique

Vectors from the synthetic fiber group (square symbol) cluster near the y-axis, while those from the natural fiber group (circle symbol) cluster near the x-axis. This demonstrate that r_{si} corresponds to synthetic fiber patterns, and r_{ni} to natural fiber patterns. Therefore, vectors from the blended fiber group (triangle symbol) lie between these clusters, demonstrating their relationships. To effectively separate these groups and determine the boundaries between them, we employ vector and geometric analysis techniques to establish two critical threshold lines: l_{t1} and l_{t2}.

In Eq. (4) and Eq. (5) as described, the two essential vectors, $\vec{s}_{xmax}$ and $\vec{b}_{xmin}$, are used in the process of establishing l_{t1}. These vectors play a pivotal role in signifying the boundaries between the synthetic and blended fabric groups.

$$\vec{s}_{xmax} = [r_{nN_s^*} \quad r_{sN_s^*}]^T \;, \qquad (4)$$
$$where \quad r_{nN_s^*} = \max_{i \in \{1,2,3\dots N_s\}} \{r_{ni}\}$$

$$\vec{b}_{xmin} = [r_{nN_b^*} \quad r_{sN_b^*}]^T \;, \qquad (5)$$
$$where \quad r_{nN_b^*} = \min_{i \in \{1,2,3\dots N_s\}} \{r_{ni}\}$$

The based vector $\vec{s}_{xmax}$ is determined on $N_s^* \in \{1,2,3 \dots N_s\}$, which represents the index of the maximum value r_{ni} within the synthetic fabric group. Similarly, the

based vector $\vec{b}_{xmin}$ is determined on $N_b^* \in \{1,2,3 \dots N_s\}$, which represents the index of the minimum value r_{ni} within the blended fabric group. After identifying these key vectors, we calculate the midpoint vector $\vec{c}_1$, which serves as the center point of our geometric approach, as described in Eq. (6):

$$\vec{c}_1 = 0.5 \times \left(\vec{s}_{xmax} + \vec{b}_{xmin}\right) \tag{6}$$

Subsequently, we create a perpendicular line to the midpoint vector $\vec{c}_1$. This line is instrumental in establishing l_{t1}, which define the boundary between the synthetic and blended fabric groups. We find the slope m_1 of the line using a component of vectors as described in Eq. (7):

$$m_1 = -\frac{\vec{b}_{xmin}(1) - \vec{s}_{xmax}(1)}{\vec{b}_{xmin}(2) - \vec{s}_{xmax}(2)} \tag{7}$$

Additionally, we define the equation of the threshold line as $l_{t1} = m_1 x + c_1$, where $0 \le x \le 1$. The y-intercept c_1 is calculated by using a component of vector $\vec{c}_1$, as described in Eq. (8):

$$c_1 = \vec{c}_1(2) - \vec{c}_1(1) \times m_1 \tag{8}$$

For the second threshold line l_{t2}, which signifies the boundary between the blended and natural fiber groups, we follow a similar procedure to create vector $\vec{b}_{ymin}$ and $\vec{n}_{ymax}$ as described by Eq. (9) and Eq. (10):

$$\vec{b}_{ymin} = [r_{nN_b^*} \quad r_{sN_b^*}]^T, \tag{9}$$

$$where \quad r_{sN_b^*} = \min_{i \in \{1,2,3 \dots N_b\}} \{r_{si}\}$$

$$\vec{n}_{ymax} = [r_{nN_n^*} \quad r_{sN_n^*}]^T, \tag{10}$$

$$where \quad r_{sN_n^*} = \max_{i \in \{1,2,3 \dots N_n\}} \{r_{si}\}$$

The based vectors: $\vec{b}_{ymin}$ is determined on $N_b^* \in \{1,2,3 \dots N_n\}$, which represents the index of the minimum value r_{si} within the blended fabric group. Conversely, the based vector $\vec{n}_{ymax}$ is determined on $N_n^* \in \{1,2,3 \dots N_n\}$, which represents the index of the maximum value r_{si} within the natural fabric group.

With these two vectors, we create l_{t2} using the same geometric analysis techniques. We calculate the slope m_2 by using the components of the vectors with the formula as described in Eq. (11):

$$m_2 = -\frac{\vec{n}_{ymax}(1) - \vec{b}_{ymin}(1)}{n_{ymax}(2) - b_{ymin}(2)} \tag{11}$$

The equation of the threshold line l_{t2} is expressed as $l_{t2} = m_2 x + c_2$, where $0 \le x \le 1$, and we compute calculate the y-intercept c_2 by using a component of vector $\vec{c}_2$, as described in Eq. (12):

$$c_2 = \vec{c}_2(2) - \vec{c}_2(1) \times m_2 \tag{12}$$

In our classification process, once the constants for l_{t1} and l_{t2} have been determined, these threshold lines play a pivotal role in the classification of unknown vectors, represented as (r_{nu}, r_{su}), into one of three distinct fiber groups: natural, synthetic, or blended fiber group. Our algorithm employs a fundamental linear equation and follows the sequence of criteria checks:

Step 1: if $r_{su} - m_1 \times r_{nu} + c_1 > 0$, classify the unknow vector into the synthetic groups. If this condition is not met, proceed to the next classification.

Step 2: if $r_{su} - m_2 \times r_{nu} + c_2 < 0$, classify the unknow vector into natural group. If this condition is not met, the unknown vector is classified into the blended group.

In this section, we have detailed our classification algorithm based on the analytic geometric technique. The algorithm's fundamental linear equations and criteria have been explained. In the next section, we will present the outcomes of applying this algorithm with training dataset, providing insights into its performance.

3.4 Results of NIR Signal Enhancement with l_p norm

Figures 7 to 9 (a) show three examples of the raw fiber spectra $\{s[n]\}$ in each group, which have the same similar pattern but exhibit variability and slight differences due to noise or bias, making it challenging to identify the group. In Figures 7 to 9 (b-c), the enhanced spectral signals $\{x_p[n]\}$ with l_p $norm$, where $p = \infty$,1 and 2, respectively, are shown and can effectively reduce spectral variability. This ensures that all signals have equal power to one.

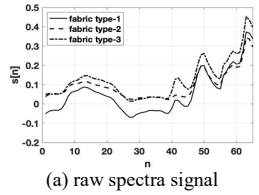

(a) raw spectra signal

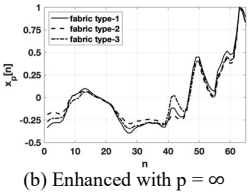

(b) Enhanced with p = ∞

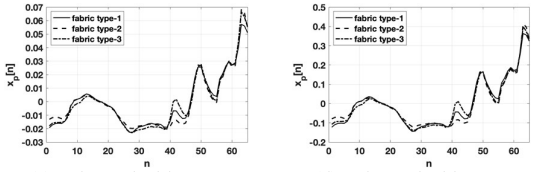

(c) Enhanced with p = 1 (d) Enhanced with p = 2

Figure 7 Signal enhancement with $l_p\ norm$ of Natural fiber group

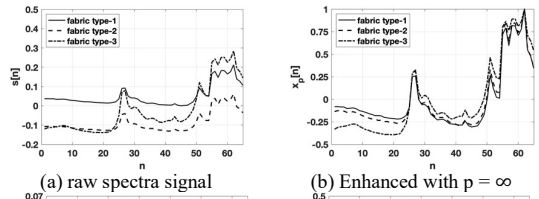

(a) raw spectra signal (b) Enhanced with p = ∞

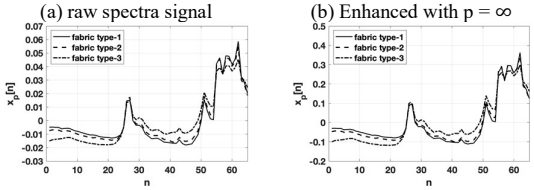

(c) Enhanced with p = 1 (d) Enhanced with p = 2

Figure 8 Signal enhancement with $l_p\ norm$ of Synthetic fiber group

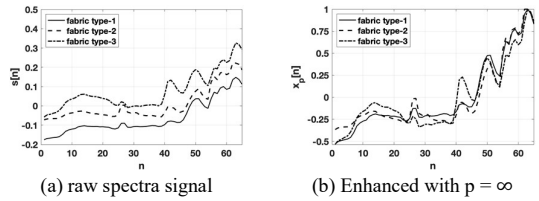

(a) raw spectra signal (b) Enhanced with p = ∞

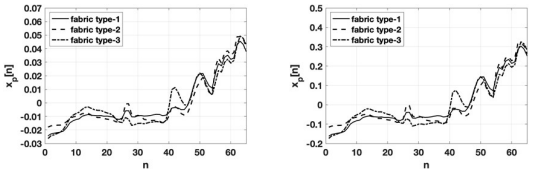

(c) Enhanced with p = 1 (d) Enhanced with p = 2

Figure 9 Signal enhancement with $l_p\ norm$ of Blended fiber group

3.5 Result of Analytic Geometric Classification with $l_p\ norm$

We extend the proposed method from Section 3 to demonstrate the use of spectral signal enhancement $\{x_p[n]\}$ with three different $l_p\ norm$ cases in the creation of new feature vectors $\vec{r}$, which extract features using the covariance-based technique. In Figures 10 (a), (b) and (c), we present vector data obtained from a 50:50 training dataset enhanced with $l_p\ norm$, where $p = \infty$,1 and 2, respectively. The figures illustrate that each $l_p\ norm$ generate a distinct threshold line l_{t1} and l_{t2}, with slight variations in the two constant values m (slop) and c (intercept) in line equation.

From Table 2 and 3, show the average values and standard deviations of the constants m_1, c_1, m_2 and c_2 for threshold line l_{t1} and l_{t2}. These values were obtained through ten random iterations on various dataset ratios. Threshold line l_{t2} demonstrates minimal variance in standard deviation values across different $l_p\ norm$ enhancements. However, the variance in standard deviations values is notably higher for threshold line l_{t1}. This variance decreases gradually as the $l_p\ norm$ shift from ∞ to 2, respectively.

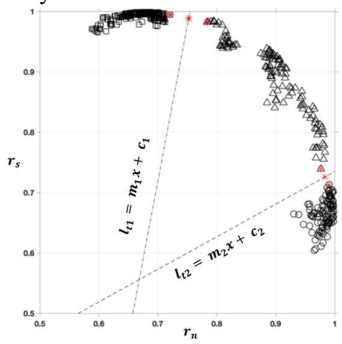

(a) Classification with $l_p - norm$ spectral enhancement, where $p = \infty$

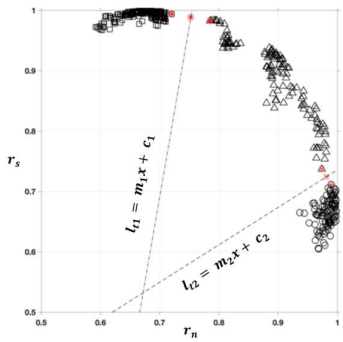

(b) Classification with $l_p - norm$ spectral enhancement, where $p = 1$

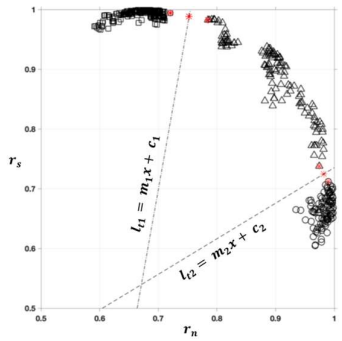

(c) Classification with $l_p - norm$ spectral enhancement, where $p = 2$

Figure 10 The new feature vector from proposed classification method with $l_p - norm$

Table 2 Average value of constants for threshold line l_{t1}

$l_p\ norm$	m_1	c_1
$p = \infty$	-10.742 ± 21.174	9.031 ± 15.882
$p = 1$	9.472 ± 14.058	-6.146 ± 10.552
$p = 2$	5.086 ± 8.104	-2.855 ± 6.078

Table 3 Average value of constants for threshold line l_{t2}

$l_p\ norm$	m_2	c_2
$p = \infty$	0.514 ± 0.111	0.227 ± 0.112
$p = 1$	0.591 ± 0.138	0.151 ± 0.139
$p = 2$	0.568 ± 0.129	0.173 ± 0.130

3.6 Results of the proposed method evaluation

To evaluate the performance of the proposed method for textile fiber classification into the natural, synthetic and blended classes, we utilize four evaluation metrics: overall accuracy, precision, and recall. These metrics are calculated using data extracted from the confusion matrix, which is generated from the classification results utilizing the test dataset with parameters obtained from the training process, unique to each iteration and acquired from ten random iterations with various dataset ratios across three different cases of $l_p\ norm$ enhancements with value of p = ∞,1 and 2. The evaluation process consists of following steps:

Step 1: Extract feature from spectral signal enhancement $\{x_p[n]\}$ using the textile template filters $\{h_p[n]\}$ for natural and synthetic, resulting in a new feature vector $\vec{r}$.

Step 2: Utilize the vector $\vec{r}$ for classification with the analytic geometric classification with constant of both threshold lines l_{t1} and l_{t2}.

Step 3: Count and record the classification results in the confusion matrix, as show in Table 4. Then, calculate the overall accuracy, precision, and recall evaluating the classification performance.

Table 4 The confusion matrix for multi-class classification.

		Actual Class		
Predicted Class	**Class**	**Natural**	**Synthetic**	**Blended**
	Natural	C_{11}	C_{12}	C_{13}
	Synthetic	C_{21}	C_{22}	C_{23}
	Blended	C_{31}	C_{32}	C_{33}

Table 4 represents a confusion matrix tailored for a multi-class classification task with three distinct classes: natural, synthetic, and blended. Within this matrix, the diagonal values C_{11}, C_{22}, and C_{33} signify *true positive* (*TP*) for each class, indicating the number of samples correctly classified within their respective classes. To calculate *false negative* (*FN*) for a specific class, look at the off-diagonal values associated with that class. For natural class, use $FN_{\text{Natural}} = C_{21} + C_{31}$. These values represent natural samples incorrectly classified as synthetic and blended, respectively. Similarly, to calculate *false positive* (*FP*) for the natural class, use $FP_{\text{Natural}} = C_{12} + C_{13}$. These values represent the instances of incorrect classifications, where samples from other classes, synthetic and blended were incorrectly classified as natural class. For a more detailed breakdown of *TP*, *FN*, *FP* and *TN* for each class shown in Table 5. The expanded information offers insights into the classification results for each class.

Table 5 The confusion matrix for multiclass classification.

	Natural	**Synthetic**	**Blended**
TP	C_{11}	C_{22}	C_{33}
FN	$C_{21} + C_{31}$	$C_{12} + C_{32}$	$C_{13} + C_{23}$
FP	$C_{12} + C_{13}$	$C_{21} + C_{23}$	$C_{31} + C_{32}$
TN	$C_{22}+C_{23}+C_{32}+C_{33}$	$C_{11}+C_{13}+C_{31}+C_{33}$	$C_{11}+C_{12}+C_{21}+C_{22}$

From Table 4, to calculate the overall accuracy, which reflects the proportion of correctly classified instances across all classes and provides an overall view of the classifier's performance, you can use the formulation as described in Eq. (13):

$$Overall\ Accuracy = \frac{\sum_{k=1}^{3} c_{kk}}{\sum_{i=1}^{3}\sum_{j=1}^{3} c_{ij}} \qquad (13)$$

Moreover, the result of overall accuracy in various of train: test ratio across three different cases three different cases of $l_p\ norm$ enhancements with value of p = ∞,1 and 2, as show in Table 6.

Table 6 Overall Accuracy across different Train: Test ratios and $l_p\ norm$ cases.

Ratio Train:Test	$p = \infty$	$p = 1$	$p = 2$
10:20	0.9995 ± 0.0006	0.9995 ± 0.0006	0.9995 ± 0.0006
20:80	0.9999 ± 0.0004	0.9999 ± 0.0004	0.9999 ± 0.0004
30:70	0.9999 ± 0.0005	0.9999 ± 0.0005	0.9999 ± 0.0005
40:60	1.0000±0.0000	1.0000±0.0000	1.0000±0.0000
50:50	1.0000±0.0000	1.0000±0.0000	1.0000±0.0000
60:40	1.0000±0.0000	1.0000±0.0000	1.0000±0.0000
70:30	1.0000±0.0000	1.0000±0.0000	1.0000±0.0000
80:20	1.0000±0.0000	1.0000±0.0000	1.0000±0.0000

In Table 6, it is demonstrated that the overall accuracy remains consistent across various $l_p\ norm$ enhancements, indicating high performance. The value of p does not significantly affect the results. Considering the lower

computational resource requirements, the $l_1\,norm$ is often preferred over the $l_2\,norm$, which involves more complex square root calculations, and the $l_\infty\,norm$, which requires finding the maximum absolute value. Therefore, the $l_1\,norm$ is an appropriate choice, especially when the method is intended for application in an embedded system, emphasizing practicality in implementation. Subsequently, we will narrow our focus to the case of $l_p\,norm$ enhancement with $p = 1$ to assess the classification performance for each individual class.

We utilize data from Table 5 to calculate the evaluation metrics of precision, recall, and accuracy for each class, and these results are presented in Tables 7 thru 9 to assess the classification performance:

Precision: measures the proportion of correctly predicted positive outcomes to all the predicted positive outcomes, with an emphasis on avoiding false positives as described in Eq. (14):

$$Precision = \frac{TP}{TP + FP} \tag{14}$$

Recall: represents the proportion of correctly predicted positive outcomes to all the outcomes in each class, focusing on the ability to avoid false negatives as described in Eq. (15):

$$Recall = \frac{TP}{TP + FN} \tag{15}$$

Accuracy: This metric measures the proportion of correctly classified instances and is defined by Eq. (16):

$$Accuracy = \frac{TP + TN}{TP + FN + FP + TN} \tag{16}$$

Table 7 Precision results across different Train:Test ratios.

Ratio Train:Test	Natural	Synthetic	Blended
10:20	0.9979±0.0027	1.0000±0.0000	1.0000±0.0000
20:80	0.9994±0.0019	1.0000±0.0000	1.0000±0.0000
30:70	0.9993±0.0021	1.0000±0.0000	1.0000±0.0000
40:60	1.0000±0.0000	1.0000±0.0000	1.0000±0.0000
50:50	1.0000±0.0000	1.0000±0.0000	1.0000±0.0000
60:40	1.0000±0.0000	1.0000±0.0000	1.0000±0.0000
70:30	1.0000±0.0000	1.0000±0.0000	1.0000±0.0000
80:20	1.0000±0.0000	1.0000±0.0000	1.0000±0.0000

Tables 7 thru 9 clearly demonstrate the exceptional performance of our proposed method, consistently achieving a perfect score of 1 for precision, recall, and accuracy in the synthetic class across various train: test ratios. This remarkable performance showcases the method's robust and reliable nature, even when dealing with a limited training dataset. However, it's important to note that when the training dataset size is below the 40:60 ratio, the precision of the natural class and the recall of the Blended class do not reach a perfect score. Consequently, this results in the overall accuracy falling short of achieving a score of one. Nevertheless, our method outperforms the approach by Ruiz et al. (2022), which involved data fusion between MIR and NIR, achieving the highest accuracy of 95% in the case study of blended fibers. Furthermore, our method surpasses the approach by Ruiz, Cantero, Riba-Mosoll, et al. (2022) who employed PCA + CVA + CNN which achieved a correct classification rate of 91.1% in the case study of blended fibers.

Table 8 Recall results across different Train:Test ratios.

Ratio Train:Test	Natural	Synthetic	Blended
10:20	1.0000±0.0000	1.0000±0.0000	0.9984±0.0021
20:80	1.0000±0.0000	1.0000±0.0000	0.9995±0.0015
30:70	1.0000±0.0000	1.0000±0.0000	0.9995±0.0017
40:60	1.0000±0.0000	1.0000±0.0000	1.0000±0.0000
50:50	1.0000±0.0000	1.0000±0.0000	1.0000±0.0000
60:40	1.0000±0.0000	1.0000±0.0000	1.0000±0.0000
70:30	1.0000±0.0000	1.0000±0.0000	1.0000±0.0000
80:20	1.0000±0.0000	1.0000±0.0000	1.0000±0.0000

Table 9 Accuracy results across different Train:Test ratios.

Ratio Train:Test	Natural	Synthetic	Blended
10:20	0.9995±0.0006	1.0000±0.0000	0.9995±0.0006
20:80	0.9999±0.0004	1.0000±0.0000	0.9999±0.0004
30:70	0.9999±0.0005	1.0000±0.0000	0.9999±0.0005
40:60	1.0000±0.0000	1.0000±0.0000	1.0000±0.0000
50:50	1.0000±0.0000	1.0000±0.0000	1.0000±0.0000
60:40	1.0000±0.0000	1.0000±0.0000	1.0000±0.0000
70:30	1.0000±0.0000	1.0000±0.0000	1.0000±0.0000
80:20	1.0000±0.0000	1.0000±0.0000	1.0000±0.0000

4. CONCLUSION

This paper introduces an innovative approach for classifying textile fibers based on near-infrared spectrum signals. The proposed method involves spectral signal enhancement using various $l_p\ norm$ values with p = ∞, 1, and 2, as a preprocessing step to assess and compare classification accuracy. The method also incorporates the textile template filters and covariance-based techniques for the feature extraction, which effectively reduces the dimensionality of spectral data into a new 2x1 feature vector. The classification is based on an algorithm rooted in the analytic geometric technique. The results show that the proposed method achieved a perfect overall accuracy of 100% when used with train and test data ratio not less than minimum at 40:60 indicating that it is robust and can generalize even when dealing with a limited training dataset. However, even under varying train and test data ratios such as 30:70, 20:80 and 10:90 ratios, the method maintains impressive accuracy values of 0.9999 ± 0.0005, 0.9999 ± 0.0004 and 0.9995 ± 0.0006, respectively. Nevertheless, this still surpasses our previous study (Yammen & Limsripraphan, 2022) where the highest accuracy achieved was 0.9922 ± 0.0078, but only when using an 80:20 training-to-test dataset ratio. These findings underscore the robustness and reliability of the proposed method in textile fiber classification across different scenarios. A notable contribution of this study is found in the simplicity and minimal computational resource demands of the proposed method, rendering it well-suited for applications in the textile industry. This is especially relevant for the embedded systems used in automating textile recycling processes or in portable devices across diverse fields that employ spectroscopy techniques. In the future work, analytical methods will be improved in predicting the composition of the blended fiber either natural or synthetic fabric.

5. ACKNOWLEDGMENT

The authors are greatly thankful to the research and researcher for industries (RRI) and the TJ Supply Limited Partnership for supporting a research grant.

6. REFERENCES

Bunchuen, S., Boonsri, U., Muneesawang P. & Yammen, S. (2011). Detection Method for Corrosion on the Pole Tip. *Naresuan University Engineering Journal, 6(2), 2011, 1-8*.

Cadzow, J. A. (2002). Minimum ℓ1, ℓ2, and ℓ∞ Norm Approximate Solutions to an Overdetermined System of Linear Equations. *Digital Signal Processing, 12(4), 524-560*. DOI:10.1006/dspr.2001.0409

Cadzow, J. A., & Yammen, S. (2002). Data Adaptive Linear Decomposition Transform. *Digital Signal Processing 12(4), 494-523*. DOI:10.1006/dspr.2001.0408

Cadzow, J. A. (1999). Linear Recursive Operator's Response Using the Discrete Fourier Transform. *IEEE Signal Processing Magazine, 16(2), 100-114*.

Cadzow, J. A. (1998). Multidimensional Recursive Linear System Synthesis. *Digital Signal Processing 8(3), 139-157*. DOI:10.1006/dspr.1998.0312

Chadalavada, K., Anbazhagan, K., Ndour, A., Choudhary, S., Palmer, W. E., Flynn, J. R., Mallayee, S., Pothu, S., Prasad, K., Varijakshapanikar, P., Jones, C., & Kholova, J. (2022). NIR Instruments and Prediction Methods for Rapid Access to Grain Protein Content in *Multiple Cereals. Sensors, 22(10), 3710*. https://doi.org/10.3390/s22103710

Chen, H., Tan, C., Lin, Z., & Wu, T. (2018). Rapid determination of cotton content in textiles by Near-Infrared spectroscopy and interval partial least squares. *Analytical Letters*, *51*(17), 2697–2709. https://doi.org/10.1080/00032719.2018.1448853

Damayanti, D., Wulandari, L. A., Bagaskoro, A., Rianjanu, A., & Wu, H. (2021). Possibility routes for textile recycling technology. *Polymers*, *13*(21), 3834. https://doi.org/10.3390/polym13213834

Da Silva BarrosM, A. C., Firmeza Ohata, E., Da Silva, S. P., Silva Almeida, J., & Reboucas Filho, P. P. (2020). An innovative approach of textile fabrics identification from mobile images using computer vision based on deep transfer learning.*2020 International Joint Conference on Neural Networks (IJCNN)*. https://doi.org/10.1109/ijcnn48605.2020.9206901

Dissanayake, G., & Weerasinghe, D. (2021). Fabric Waste Recycling: a Systematic Review of Methods, Applications, and Challenges. Materials Circular Economy, 3(1). https://doi.org/10.1007/s42824-021-00042-2

Du, X., Wang, J., Dong, D., & Zhao, X. (2019). Development and Testing of a Portable Soil

Nitrogen Detector Based on Near-infrared Spectroscopy. IEEE Joint International Information Technology and Artificial Intelligence Conference. https://doi.org/10.1109/itaic.2019.8785499

Filho, W. L., Perry, P., Heim, H., Dinis, M. a. P., Moda, H. M., EbhE. E., & Paço, A. M. F. D. (2022). An overview of the contribution of the textiles sector to climate change. *Frontiers in Environmental Science*, *10*. https://doi.org/10.3389/fenvs.2022.973102

Fuangpian, T., Muneesawang P., & Yammen S. (2011). An Algorithm for Detection of Solder Balls on HGA. *Naresuan University Journal, Special Issue,.24–32*.

Giussani, B., Escalante-Quiceno, A. T., Boqué, R., & Riu, J. (2021). Measurement Strategies for the Classification of Edible Oils Using Low-Cost Miniaturised Portable NIR Instruments. Foods, 10(11), 2856. https://doi.org/10.3390/foods10112856

Guifang, W., Hai, M., & Xin, P. (2015). Identification of varieties of natural textile fiber based on Vis/NIR spectroscopy technology. In IEEE Advanced Information Technology, Electronic and Automation Control Conference. https://doi.org/10.1109/iaeac.2015.7428621

Habibullah, M., Oninda, M. a. M., Bahar, A. N., Dinh, A., & Wahid, K. A. (2019). NIR-Spectroscopic Classification of Blood Glucose Level using Machine Learning Approach. Canadian Conference on Electrical and Computer Engineering. https://doi.org/10.1109/ccece.2019.8861843

Limsripraphan W., & Yammen, S. (2022). Signal Enhancement for Natural Fiber Textile Classification Algorithm. *Proceedings of the 18th Naresuan Research Conference: Steering towards Frontier University: Challenges and Foresight* (*NRC18*). http://conference.nu.ac.th/nrc18/

McVey, C., McGrath, T. F., Haughey, S. A., & Elliott, C. T. (2021). A rapid food chain approach for authenticity screening: The development, validation and transferability of a chemometric model using two handheld near infrared spectroscopy (NIRS) devices. Talanta,222,121533. https://doi.org/10.1016/j.talanta.2020.121533

Ruiz, J. R., Cantero, R., & Puig, R. (2022). Classification of textile samples using data fusion combining near- and Mid-Infrared spectral information. *Polymers*, *14*(15), 3073. https://doi.org/10.3390/polym14153073

Ruiz, J. R., Cantero, R., Riba-Mosoll, P., & Puig, R. (2022). Post-Consumer Textile Waste Classification through Near-Infrared Spectroscopy, Using an Advanced Deep Learning Approach. *Polymers*, *14*(12), 2475. https://doi.org/10.3390/polym14122475

Sun, X., Zhou, M., & Sun, Y. (2015). Classification of textile fabrics by use of spectroscopy-based pattern recognition methods. *Spectroscopy Letters*, *49*(2), 96–102. https://doi.org/10.1080/00387010.2015.1089446

Yammen, S., & Limsripraphan, W. (2022). Matched Filter Detector for Textile Fiber Classification of Signals with Near-Infrared Spectrum. 2022 Asia-Pacific Signal and Information Processing Association Annual Summit and Conference (APSIPA ASC). https://doi.org/10.23919/apsipaasc55919.2022.9980054

Yammen, S., & Muneesawang, P. (2021). P. 2014. An Advanced Vision System for the Automatic Inspection of Corrosions on Pole Tips in Hard Disk Drives. *IEEE Transactions on Components, Packaging and Manufacturing Technology, 4(9), 1523-1533*.

Zhou, J., Yu, L., Ding, Q., & Wang, R. (2019). Textile Fiber Identification Using Near-Infrared Spectroscopy and Pattern Recognition. Autex Research Journal, 19(2), 201–209. https://doi.org/10.1515/aut-2018-0055

Piribauer, B., & Bartl, A. (2019). Textile recycling processes, state of the art and current developments: A mini review. *Waste Management & Research*, *37*(2), 112–119. https://doi.org/10.1177/0734242x18819277

7. BIOGRAPHIES

Wachira Limsripraphan received the bachelor's and master's degree in computer science, Currently, studying for a Ph.D. program in computer engineering from Naresuan University, Phitsanulok, Thailand. He is also employed as an instructor in computer engineering at Pibulsongkram Rajabhat University.

Dr. Suchart Yammen received the bachelor's (2nd Honor with class rank one) degree in electrical engineering from Chiang Mai University, Chiang Mai, Thailand, in 1988, and the M.S. and Ph.D. degrees from Vanderbilt University, Nashville, TN, USA, in 1998 and 2001, respectively. He was a supervisor of the Colgate-Palmolive (Thailand) Company, Ltd., Bangkok, Thailand in 1988, and also served as production engineer in the powder plant. From 1989 to 1993, he was with Siam Cement Public Company, Ltd., Bangkok, not only as a production engineer, a maintenance engineer but also a project engineer. In 1994, he also joined with Naresuan University, Thailand, where he is also currently an associate professor of electrical engineering, he was an assistant to the president for administrative affairs and for information technology, and the Engineering Dean. Furthermore, he is one of the two authors to produce the textbook title: "The Era of Interactive Media" (New York, USA: Springer Publisher, 2012), and has co-authored of the textbook title: *Principles of Communications* (Bangkok, Thailand: Chulalongkorn University Press: CUP, 2011). His current research interests also include various areas of a power electrical engineering, digital signal processing and analysis, automatic control systems, and the related areas in biomedical engineering, computer engineering, renewable energy, energy conservation management, robotics, system identification and modeling.
Dr. Yammen also is various famous professional members, i.e., an IEEE Senior Member, a Fellow Member of the Engineering Institute of Thailand (EIT), Associate Member of Council of Engineers (COE), and the Director for the Research Unit of Biomedical Engineering and Innovation for Social Equality (BEISE) at Faculty of Engineering in Naresuan University, Phitsanulok, Thailand. etc.